Parametric Analysis of Acral Lesions on Dermoscopy

Hitoshi Iyatomi∗, Hiroshi Oka†, Masaru Tanaka⋆, and Koichi Ogawa∗

∗ Department of Electrical Informatics, Hosei University Faculty of Engineering (Tokyo, JAPAN).
† Department of Information and Computer Science, Keio University Faculty of Science and Technology (Yokohama, JAPAN).
⋆ Department of Dermatology, Tokyo Women's Medical University Medical Center East (Tokyo, JAPAN).
∗ 3-7-2 Kajino-cho Koganei, 184-8584, Tokyo.
∗ (Tel) +81-42-387-6217 (FAX) +81-42-387-6381
(e-mail) iyatomi@hosei.ac.jp

***Abstract*— A half of melanomas in non-white populations are from acral volar area and an appearance of these lesions is completely different from that of other parts of lesions. However, no research for classifying these lesions has been conducted. In this paper, we describe a diagnosis classifier of acral volar melanomas. We used our dermatologist-like tumor area extraction algorithm and extracted a total of 428 features from 199 acral dermoscopic images (169 nevi and 30 melanomas) and built a linear classifier. Our classifier selected 17 features and achieved a sensitivity of 90.0%, a specificity of 92.3% and an area under the ROC curve (AUC) value of 0.944 using a leave-one-out cross-validation strategy.**

I. Introduction

Although advanced malignant melanoma is often intractable, early-stage melanoma is curable in many cases, particularly when metastases are not present. Therefore, early detection and diagnosis of melanoma is essential to the reduction of melanoma-related deaths. However, it is often difficult to distinguish between early-stage melanoma and nevi with the naked eye, especially when small lesions are involved.

In 1987, Soyer *et al.* [1] developed Dermoscopy, which consists of uniformly illuminated magnifier with deflecting plate to improve diagnostic accuracy of pigmented skin lesions (PSLs). However, diagnosis of PSLs with dermoscopy is often subjective and is therefore associated with poor reproducibility and errors. Despite the use of dermoscopy, the accuracy of melanoma diagnosis by expert dermatologists is still estimated to be 75-84% [2]. Several groups have developed automated analysis procedures to overcome these problems and reported high levels of diagnostic accuracy [3]-[13]. Rubegni *et al.* [6] achieved a sensitivity (SE) of 94.3 % and a specificity (SP) of 93.8% on 350 cases of nevi and 200 cases of malignant melanoma. Recently, Celebi *et al.* [13] achieved a SE of 93.3% and a SP of 92.3% based on 476 cases of nevi and 88 cases of melanomas with their wise controlled tumor area detection algorithm and support vector machines with radial basis function (RBF) kernel. However, several problems have persisted with these software-based approaches. For example, results obtained from these studies are not comparable because different images were used in each study. In addition, these studies were designed to develop a screening system for new patients using standalone systems and therefore they have not been open to the public.

In such background, we have developed an Internet-based melanoma screening system [14]. The URL of the site was changed and it is now http://dermoscopy.k.hosei.ac.jp. When one send a dermoscopy image from a commonly used computer to this system with corresponding clinical data, the system extracts tumor-areas, calculates the characteristics and generates a diagnosis by a diagnostic classifier. The latest version of our system (Mar.2007) equips the dermatologist-like tumor area extraction algorithm that achieved superior extraction performance [15][16] and a neural network classifier. The system achieved the classification accuracy of 85.9% in SE and 86.0% in SP using a leave-one-out cross-validation stragegy of 1258 dermoscopy images (1060 melanocytic nevi and 198 melanomas).

In non-white populations, it is specific but almost a half of melanomas are found in acral (palm and sole) area [17]. An appearance of these acral lesions is completely different to that of others and different clinical findings are used for diagnosing them. Fig. 1 shows samples of dermoscopy images of common (not acral) and acral lesions. The top-left image is a sample of common nevus. The top-right image is one of typical acral nevus and bottom-right is typical acral melanoma. For acral lesions, parallel-ridge pattern (ridge areas of lesion are selectively pigmented) indicates the malignancy and parallel-furrow pattern (furrow areas of lesion are selectively pigmented) does the benignity [2]. This is very effective clinical strategy and it is reported that the diagnosis accuracy of this is reported to around 86% in SE %[18]. However, acral lesion sometimes have fibrillar like pattern (called "fibrillar pattern") shown in lower-left of Fig. 1 and this makes difficult of diagnosis. Extraction and/or quantitative evaluation of these parallel patterns are also difficult by the computer-based image analysis and therefore only few research on this topic have been made even though acral melanoma is specifically dominant melanoma for non-white populations.

In this paper, we developed a classifier of acral lesions for our Internet-based melanoma diagnosis system. Our method

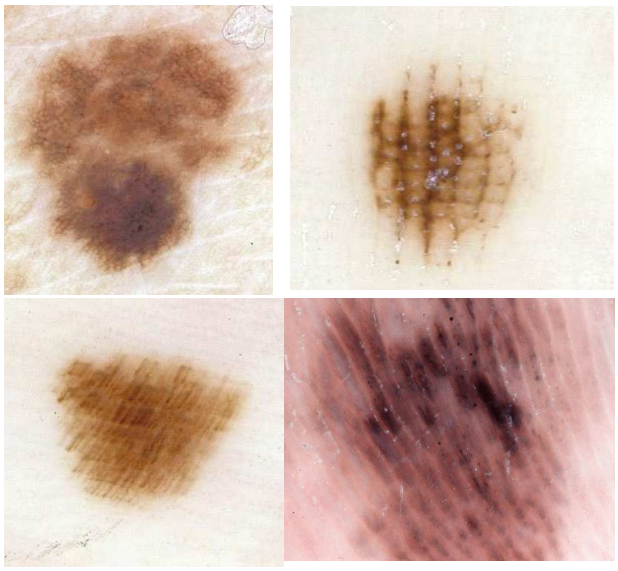

Fig. 1. Examples of dermoscopy images
from top-left: Clark nevus (common benign), acral benign.
from bottom-left acral fibrillar pattern (benign) and acral melanoma

parameterizes the PSL objectively and calculates the degree of the malignancy from these parameters automatically. Therefore, the proposed method does not require the extraction and evaluation of parallel patterns, the typical dermoscopic structures directly.

II. Materials and methods

A. Materials

Dermoscopic digital acral images of PSLs were collected from three countries (Japan, Italy, and Austria). All digital images of PSLs were 24bit colored, large enough images stored in jpeg format and they were reduced the size in 40 pixels/mm. A total of 199 acral dermoscopy images; 169 benign nevi and 30 melanomas were used in this study. Most of these cases were diagnosed based on pathological examination of biopsy material and remaining cases were diagnosed clinically by several expert dermatologists. These established results were used as gold standard (training data) for building the classifier.

B. Method

1) Tumor area extraction: Diagnostic accuracy highly depends on the accurate extraction of the tumor area and therefore it is very important step for building a computer-based diagnosis system. We used our "dermatologist-like" tumor area extraction algorithm [15] that combines both pixel-based and region-based methods and introduces a region-growing approach that aims to bring the automatic extraction results closer to those determined by dermatologists. In our previous research, we confirmed that this method achieved superior performance to conventional ones [15][16].

2) Feature selection: After extracting the tumor area, we rotated the tumor object to align its major axis with the Cartesian x-axis. Then, we calculated a total of 428 image related objective features with reference to the ABCD rule [19] and clinical strategies for acral volor lesions, parallel-ridge and parallel-furrow pattern [17][18]. ABCD rule refers to asymmetry, border sharpness, color variegation, and differential structures. The D of ABCD rule evaluates the existence dermoscopic features such as pigment networks, branched streaks, structureless area, dots, and globules. It is desirable to calculate features to represent these structures directly. However, extracting these features is often difficult because of the vast variety of dermoscopy images and the highly subjective definitions of these criteria. Argenziano *et al.* reported that the inter-observer agreement for these features was not high even among expert dermatologists [20]. Therefore, in this study, we extracted texture features such as skewness, energy, moment, entropy and correlation of red, green and blue channels for the whole lesion area and the peripheral lesion area to quantify the D components.

The calculated features can be roughly categorized into color, symmetry, border and texture properties. As color related features, a total of 140 parameters were calculated: minimum (min), average (ave), maximum (max), standard deviation (SD) and skewness (skew) value in the RGB and HSV color space, respectively (subtotal 30) for the whole tumor area (tumor), periphery of the tumor area (peripheral), differences between the tumor area and the surrounding normal skin (tumor-skin) and that between peripheral and normal-skin (peripheral-skin). In addition, a total of 20 color related features were calculated; the number of colors in the tumor area and peripheral tumor area in the RGB and HSV color spaces quantized to 8^3 and 16^3 colors, respectively (subtotal 8), the average color of normal skin (R, G, B, H, S, V: subtotal 6), and average color differences between the peripheral tumor area and inside of the tumor area (R, G, B, H, S, V subtotal 6). Note that the peripheral part of the tumor is defined as the region inside the border that has an area equal to 30% of the tumor area.

In the symmetry category, a total of 80 features were calculated. We designed 10 intensity thresholds values from 5 to 230 with a stepsize of 25. In the extracted tumor area, thresholding was performed and the areas whose intensity was lower than the threshold were determined. From each such area, we calculated 8 features as follows: area ratio to original tumor size, circularity, differences of the center of gravity between original tumor (Δ_x, Δ_y), standard deviation of the distribution (σ_x, σ_y) and skewness of the distribution (σ_x^3, σ_y^3).

In order to quantify the border structure, a total of 32 features were calculated. The tumor areas are divided into eight equi-angle regions. In each region, we defined a window whose size is $S_B \times S_B$ and its center is a pixel of the border of the tumor. In each window, a ratio of color intensity between inside and outside of the tumor and a gradient of color intensity were calculated in the blue and luminance channels (ratio: B_B and B_L, gradient: B_{Δ_B} and B_{Δ_L}), respectively. They are averaged for all 8 regions (subtotal 4). We calculated four features each from eight different window size S_B; 1/5, 1/10,

1/15, 1/20, 1/25, 1/30, 1/35 and 1/40 of the length of the major axis of the dermoscopy image.

As for the texture features, a of total 176 parameters were calculated. We prepared 11 different sized co-occurrence metrics with distance value δ ranging from 1/2 to 1/64 of the length of the major axis of the dermoscopy image. Based on each co-occurrence matrix, energy, moment, entropy and correlation were calculated for in four directions (0, 45, 90 and 135 degrees).

These 428 image features were transformed into [0, 1] range using z-score normalization. We calculated the correlation among all features and all combinations whose absolute correlation coefficient exceeds 0.99 were eliminated except one representative in order to build a robust regression model. On the other hand, the training signal of 1 and -1 were assigned to each case of melanoma and nevus, respectively. Finally, we performed incremental stepwise input selection with Wilks' lambda hypothesis test [21] to select an effective set of features.

3) classification and evaluation criteria: We build a linear classifier with selected features. We evaluated the accuracy of the built classifier with a sensitivity (SE) and a specificity (SP) criteria using a leave-one-out cross-validation strategy. We also plotted the receiver operating characteristic (ROC) curve to examine the classifier performance under varying conditions. The diagnostic performance was also quantified by the area under the ROC curve (AUC) measure. The AUC value ranges from 0 to 1 and it is closer to 1, the higher the classification performance is represented.

III. Results

After elimination of high correlated features, a total of 202 features were remained. The incremental stepwise input selection method selected regression model with 17 features. The summary of the selected features are in Table I. The developed linear model with selected 17 features attained a standard deviation of mean square error ($\bar{E}$) of 0.400 and the determination coefficient adjusted by degree of freedom (R^2) was 0.680.

The typical diagnostic accuracy of the model was 90.0% in SE, 92.3% in SP and an AUC value was 0.944 with the leave-one-out cross-validation test. Fig. 2 shows the ROC curve.

On the other hand, a developed linear classifier with 10 features ($1 \leq$ ID ≤ 10) achieved almost equivalent classification performance; 90.0% in SE, 91.1% in SP and an AUC value was 0.934 using the leave-one-out cross-validation test.

IV. Discussion

Assessing the presence of parallel-ridge pattern is very effective clinical finding for diagnosing acral volar melanoma [17][18] and is widely used. We can therefore consider it is reasonable to make a computer-based diagnostic system to detect these features for diagnosing these lesions. Acral volar dermoscopy images, however, sometimes have complicated appearances, such as fibrillar pattern, lattice-like pattern and so on and it is often required experience and/or knowledge to identify parallel-ridge or parallel-furrow pattern. It is desirable

TABLE I

Selected 17 features by stepwise input selection stragegy

ID	Category	Features		
1	asymmetry	circularity	$V \leq 55$	
2	color	average	Saturation	normal skin
3	color	max	B	tumor-normal skin
4	texture	energy	0 deg	δ= 1/64 of image size
5	color	average	Hue	peripheral-normal skin
6	asymmetry	Δ_x	$V \leq 55$	
7	texture	correlation	90 deg	δ= 1/11 of image size
8	asymmetry	circularity	$V \leq 80$	
9	texture	energy	135 deg	δ= 1/2 of image size
10	color	average	Green	normal skin
11	asymmetry	Δ_x	$V \leq 30$	
12	color	skweness	Saturation	tumor
13	texture	correlation	135 deg	δ= 1/2.8 of image size
14	asymmetry	σ_x	$V \leq 155$	
15	color	minimim	S	tumor-normal skin
16	asymmetry	Δ_y	$V \leq 30$	
17	texture	correlation	90 deg	δ= 1/2 of image size

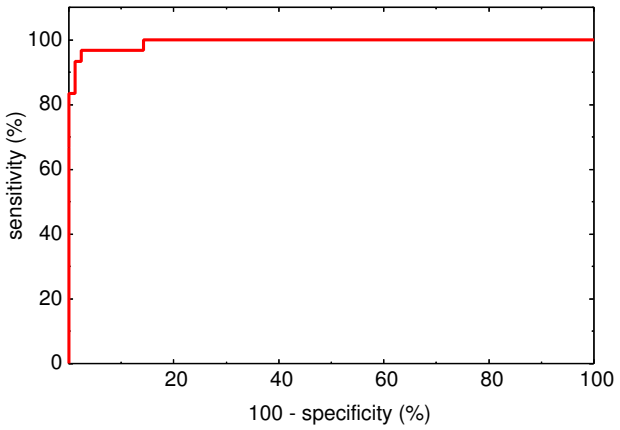

Fig. 2. ROC curves for diagnostic threshold in the detection of acral melanomas.

to calculate features to represent these structures directly. However, extracting these features is often difficult because of the vast variety of dermoscopy images and the highly subjective definitions of these criteria. Detection and evaluation of parallel patterns observed in acral volar dermoscopy image by top-down image analysis with knowledge of dermatologists are difficult in many cases. This is the reason that even though acral volar melanoma is dominant one for non-white populations, only little research for an automatic diagnosis for these lesions have been made.

Our regression model achieved very high diagnostic accuracy. We can consider that our classifier recognizes the dermoscopic characteristics of acral lesion image appropriately. The selected 17 features shows rather different trend compared with classifying general (non acral) pigmented skin lesions. Classifying a general dermoscopy image requires focusing mainly in color property of the tumor. With this experiment, we found the circularity and distribution of dark pigmented area (under the intensity of 55/255 and 30/255) were effective features to diagnose acral melanomas.In addition, the energy from texture property in higher resolution and standard deviation of hue in tumor area are also considered important for

diagnosing them.

Although good recognition accuracy was obtained, the number of the tested image is limited. We keep collecting data and develop a robust classifier.

V. Conclusions

In this paper, we developed a diagnosis classifier for acral lesions for finding early stage of acral melanomas specifically seen in non-white populations. We extracted a total of 428 image features from 199 acral dermoscopy images and built a linear regression model. We confirmed our linear model achieved the sensitivity of 90.0% and the specificity of 92.3% using the leave-one-out cross-validation strategy. We will mount a refined model of the proposed classifier on our Internet-based melanoma screening system in near future.

Acknowledgment

This research was partially supported by the Ministry of Education, Science, Sports and Culture Grant-in-Aid for Young Scientists program (B), 17790788, 2005-2006.

References

[1] H.P.Soyer, J.Smolle, H.Kerl and H.Stettnre, "Early diagnosis of malignant melanoma by surface microscopy," Lancet, Vol.2, p.803, 1987.

[2] W.Stolz, O.B.Falco, P.Bliek, M.Kandthaler, W.H.C.Burgdorf and A.B.Cognetta, "Color Atlas of Dermatoscopy – 2nd enlarged and completely revised edition," Berlin, Blackwell publishing, 2002.

[3] H.Ganster, A.Pinz, R.Roehrer, E.Wilding, M.Binder and H.Kitter, "Automated melanoma recognition," IEEE Trans. on Medical Imaging, Vol.20, No.3, pp.233-239, Mar. 2001.

[4] P.Rubegni, M.Burroni, G.Cevenini, R.Peorotti, G.Dell'Eva, P.Barbini et.al, "Digital dermoscopy analysis and artificial neural network for the differentiation of clinically atypical pigmented skin leisos: a retrospective study," Journal of investigate of Dermatology, Vol.119, pp.471-474, 2002.

[5] A.Blum, H.Luedtke, U.Ellwanger, R.Schwabe, G.Rassner and C.Garbe, "Digital image analysis for diagnosis of cutaneous melanoma. Development of a highly effective computer algorithm based on analysis of 837 melanocytic lesions," British Journal of Dermatology, Vol.151, pp.1029-1038, 2004.

[6] P.Rubegni, G.Cevenini, M.Burroni, R.Perotti, G.Dell'Eva, P.Sbano et.al, "Automated diagnosis of pigmented skin lesions," International Journal of Cancer, Vol.101, pp.576-580, 2002.

[7] K.Hoffman, T.Gambichler, A.Rick et al, "Diagnostic and neural analysis of skin cancer (DANAOS). A multicentre stidy for collection and computer-aided analysis of data from pigmented skin lesions using digital dermoscopy," British Journal of Dermatology, Vol.149, pp.801-809, 2003.

[8] M.Burroni, P.Sbano, G.Cevenini, M.Risulo, G.Dell'Eva, P.Barbini, C.Miracco, C.Miracco, M.Fimiani, L.Andreassi and P.Rugegni, "Dysplastic naevus vs. in situ melanoma: digital dermoscopy analysis," British Journal of Dermatology, Vol.152, pp.679-684, 2005.

[9] S.Seidenari, G.Pellacani and C.Grana, "Pigment distribution in melanocytic lesion images: a digital parameter to be employed for computer-aided diagnosis," Skin Research and Technology, Vol.11, pp.236-241, 2005.

[10] Menzies SW, Bischof L, Talbot H, et al, "The performance of SolarScan - An. automated dermoscopy image analysis instrument for the diagnosis of primary melanoma," ARCHIVES OF DERMATOLOGY, Vol.141, No.11, pp.1388-1396, NOV. 2005.

[11] M.Mastrolonardo, E.Conte, J.P.Zbilut J.P, "A fractal analysis of skin pigmented lesions using the novel tool of the variogram technique," Chaos solutions and fractals, Vol.28, No.5, pp.1119-1135, 2006.

[12] S.Seidenari,G.Pellacani,C.Grana C, "Asymmetry in dermoscopic melanocytic lesion images: a computer description based on colour distribution," Acta dermato-venereologica, Vol.86, No.2, pp. 123-128, 2006.

[13] M.E.Celebi, H.A.Kingravi, B.Uddin, H.Iyatomi, Y.A.Aslandogan, W.V.Stoecker, and R.H.Moss, "A methodological approach to the classification of dermoscopy images," Computerized Medical Imaging and Graphics, 2007. (In press)

[14] H.Oka, M.Hashimoto, H.Iyatomi and M.Tanaka, "Internet-based program for automatic discrimination of dermoscopic images between melanoma and Clark nevi," British Journal of Dermatology, No.150, 5, p.1041, 2004.

[15] H.Iyatomi, H.Oka, M.Tanaka et.al, "Quantitative assessment of tumour area extraction from dermoscopy images and evaluation of the computer-based methods for automatic melanoma diagnostic system," Journal of Melanoma Research, Vol.16, No.2, pp.183-190, 2006.

[16] M.E.Celebi, Y.A.Aslandogan, W.V.Stoecker, H.Iyatomi, H.Oka, X.Chen, "Unsupervised border detection in dermoscopy images, " Skin Research and Technology, 2007 (accepted).

[17] T.Saida, S.Oguchi, A.Miyazaki, "Dermoscopy for acral pigmented skin lesions," Clinics in Dermatology, Vol.20, pp.279-285, 2002.

[18] T.Saida, A.Miyazaki, S.Oguchi et.al, "Significance of Dermoscopic Patterns in Detecting Malignant Melanoma on Acral Volar Skin," Arch Dermatol, Vol.140, pp.1233-1238, 2004.

[19] W.Stolz, A.Riemann, A.B.Cognetta, L.Pillet *et al,* "ABCD rule of dermatoscopy: a new practical method for early recognition of malignant melanoma," European Journal of Dermatology, No.4, pp.521-527, 1994.

[20] G.Argenziano H.P.Soyer, S.Chimenti et.al, "Dermoscopy of pigmented skin lesions: Results of a consensus meeting via the Internet," Journal of Academy of Dermatology, Vol.48, No.5, pp.679-693, May, 2003.

[21] B.S.Everitt and G.Dunn, Applied Multivariate Data Analysis, London: Edward Arnold, pp.219-220, 1991.